Geometric Preferences of Tricobalt Clusters Having 47−49 Valence Electron Counts: Deceptively Simple Cyclic Voltammetric Responses and EPR Evidence for Exchange-Coupled Dimers in Frozen Solutions†

Matthew P. Robben,‡ Philip H. Rieger,*,§ and William E. Geiger*,‡

Contribution from the Departments of Chemistry, University of Vermont, Burlington, Vermont 05405, and Brown University, Providence, Rhode Island 02912

Received September 18, 1998

Abstract: Oxidations and reductions of a series of 48-electron (e^-) metal clusters containing a tricobalt core have been investigated by voltammetry, electrolysis, IR spectroelectrochemistry, and EPR spectroscopy. Three isomers of $Cp_3Co_3(CO)_3$ have been studied. The all-CO-bridging isomer C_{3v} $Cp_3Co_3(\mu\text{-}CO)_3$ (**1B**) is stable in the 48 e^- and 49 e^- forms, but the 47 e^- cation isomerizes to a doubly-CO-bridging structure $\mathbf{1T}^+$. The other two isomers, $Cp_3Co_3(\mu_3\text{-}CO)(\mu\text{-}CO)_2$ (**1F**) and $Cp_3Co_3(\mu\text{-}CO)_2(CO)$ (**1T**), are present in about a 1:1 ratio near room temperature, but their solutions show only Nernstian 1 e^- cyclic voltammetry (CV) responses. IR spectroelectrochemistry and analysis of the $E_{1/2}$ values show that the deceptively simple CV responses arise from a rapid equilibration between isomers **1F** and **1T**, rather than from a lack of structural change accompanying charge transfer. The cluster $Cp^*_2Cp'Co_3(\mu_3\text{-}CO)(\mu\text{-}CO)_2$ (**3**) ($Cp^* = C_5Me_5$, $Cp' = C_5MeH_4$) is shown to retain its isomeric identity through three cluster oxidation states, most likely owing to a steric preference for a face-bridging carbonyl ligand in the ring-substituted complex. The 49 e^- anions of the tricobalt complexes display EPR spectra consistent with a SOMO which is antibonding in the trimetallic plane. Additional regular hyperfine features in glassy matrices at 77 K are assigned to dimers consisting of a 49 e^- anion magnetically coupled to either a 48 e^- neutral precursor or another 49 e^- anion.

Introduction

Easily deformed metal clusters are of interest in terms of both their fluxional and isomerization processes.[1,2] Although studies of homoleptic metal carbonyls have dominated this research area, a class of compounds in which groups of three carbonyl ligands are replaced by isolobal[3] cyclopentadienyl anions (Cp) has also received a great deal of attention.[4,5] The latter complexes, having metal-to-CO ratios of approximately unity, may be relevant as models of small molecules such as carbon monoxide adsorbed onto metal surfaces.[6]

The family of 48-electron (e^-) ("electron precise") complexes of stoichiometry $(\eta^5\text{-}C_5R_5)_3M_3(CO)_3$, where M = Co, Rh, and Ir, has been intensely studied regarding how the metal−carbonyl bonding is affected by the nature of the metal, the substitution in the cyclopentadienyl ring, and even the physical state of the sample. The four different types of isomers isolated for $Cp_3M_3(CO)_3$[4,5] are shown in Chart 1.

Our experimental interest has involved the structural preferences of odd-electron species derived from the 48 e^- precursors. Made more difficult by the normal absence of NMR data for the paramagnetic species, studies have nevertheless identified electron-transfer-induced isomerizations, in some cases accompanied by remarkable increases in isomerization rates.[8] For example, the 47 e^- species of type **T** isomerize to type **B** isomers at rates as much as 10^8 higher than in the 48 e^- species when $M_3 = Rh_3$[8a,b] or $IrCo_2$[8c] (Chart 1).

The present paper contains an examination of the lightest member of this series, namely $Cp_3Co_3(CO)_3$ (**1**). Prepared by photolysis of $CpCo(CO)_2$, this trinuclear system shows a fascinating degree of flexibility, and a number of papers[9−14] have been necessary to clarify that (i) the stable crystalline form contains one face-bridging CO and two edge-bridging carbon-

† Structural Consequences of Electron-Transfer Reactions, Part 35. Part 34: Shaw, M. J.; Geiger, W. E.; Hyde, J.; White, C. *Organometallics* **1998**, *17*, 1169.

‡ University of Vermont.

§ Brown University.

(1) Cotton, F. A. *J. Organometallic Chem.* **1975**, *100*, 29.

(2) (a) Johnson, B. F. G.; Benfield, R. E. In *Transition Metal Clusters*; Johnson, B. F. G., Ed.; John Wiley and Sons: Chichester, U.K., 1980; Chapter 7. (b) Johnson, B. F. G.; Rodgers, A. In *The Chemistry of Metal Cluster Complexes*; Shriver, D. F., Kaesz, H. D., Adams, R. D., Eds.; VCH Publishers: New York, 1990; Chapter 6.

(3) Collman, J. P., Hegedus, L. S., Norton, J. R., Finke, R. G., Eds. *Principles and Applications of Organotransition Metal Chemistry*; University Science Books: Mill Valley, CA, 1987; p 52.

(4) Reviewed in: Wadepohl, H.; Gebert, S. *Coord. Chem. Rev.* **1995**, *143*, 535.

(5) Braga, D.; Grepioni, F.; Wadepohl, H.; Gebert, S.; Calhorda, M. J.; Veiros, L. F. *Organometallics* **1995**, *14*, 5350.

(6) Mercandelli, G. P.; Sironi, A. *J. Am. Chem. Soc.* **1996**, *118*, 11548.

(7) Muetterties, E. L. *Chem. Rev.* **1979**, *79*, 91.

(8) (a) Mevs, J. M.; Geiger, W. E. *J. Am. Chem. Soc.* **1989**, *111*, 1922 (b) Mevs, J. M.; Gennett, T.; Geiger, W. E. *Organometallics* **1991**, *10*, 1229 (c) Geiger, W. E.; Shaw, M. J.; Weunsch, M.; Barnes, C. E.; Foersterling, F. H. *J. Am. Chem. Soc.* **1997**, *119*, 2804.

(9) King, R. B. *Inorg. Chem.* **1966**, *5*, 2227.

(10) Vollhardt, K. P. C.; Bercaw, J. E.; Bergman, R. G. *J. Organomet. Chem.* **1975**, *97*, 283.

(11) Lee, W. S.; Brintzinger, H. *J. Organomet. Chem.* **1977**, *127*, 87.

(12) Cotton, F. A.; Jamerson, J. D. *J. Am. Chem. Soc.* **1976**, *98*, 1273.

(13) Bailey, W. I., Jr.; Cotton, F. A.; Jamerson, J. D.; Kolthammer, B. W. S. *Inorg. Chem.* **1982**, *21*, 3131.

(14) Robben, M. P.; Geiger, W. E.; Rheingold, A. L. *Inorg. Chem.* **1994**, *33*, 5615.

10.1021/ja983341+ CCC: $18.00
Published on Web 12/29/1998

Chart 1

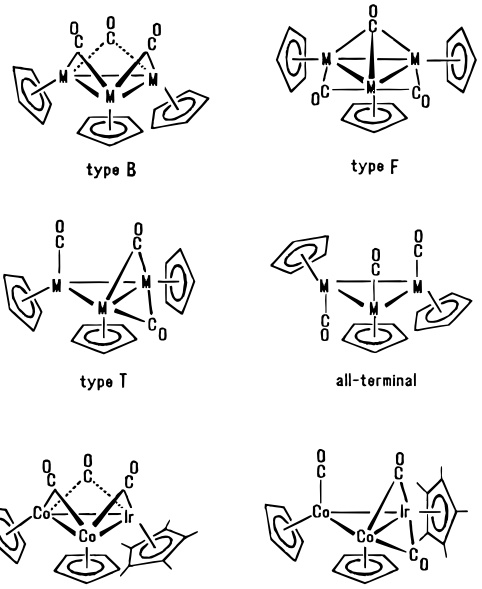

Chart 2

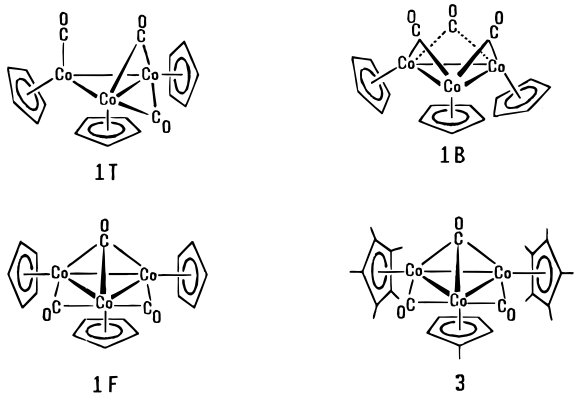

yls[12,13] (isomer **1F**, our nomenclature[15] highlighting the *f*ace-bridging carbonyl), (ii) its solutions generally contain a mixture of **1F** and an isomer **1T** having one *t*erminal CO and two edge-bridging carbonyls[10−15] [the all-terminal tricarbonyl isomer (Chart 2) is found only for $Cp_3Ir_3(CO)_3$[16] and is not a factor here], and (iii) the all-edge-bridging isomer **1B** having idealized C_{3v} symmetry may also be isolated from the photolysis reaction.[14]

In this paper, we quantify the equilibrium between isomers **1F** and **1T**, also addressing the claim that **1F** is the exclusive isomer in nonpolar solvents.[12,13] We show that voltammetry of isomeric mixtures of **1F** and **1T** is deceptive in that it hides the fact that two isomers are present under electrochemical conditions. We also describe the 1 e^- reductions and oxidations of both isomer **1B** and the mixture **1F**/**1T**, discussing the evidence for electron-transfer-induced isomerization reactions in the odd-electron systems. Included is a study of two Cp-derivatized complexes known to retain one isomeric form in both solution and the solid state as 48 e^- complexes:[17] $Cp^*Cp'_2Co_3(\mu_3\text{-CO})(\mu\text{-CO})_2$ (**2**) and $Cp^*_2Cp'Co_3(\mu_3\text{-CO})(\mu\text{-CO})_2$ (**3**) (Cp' = C_5MeH_4, Cp^* = C_5Me_5). Along with $Cp'_3Co_3(\mu_3\text{-CO})(\mu\text{-CO})_2$,[17] these complexes are important in showing that substitution of −H by $-CH_3$ in the cyclopentadienyl rings tips the scale in favor of the face-bridging form **1F**. We find that this isomer is retained throughout the 47 e^-/48 e^-/49 e^- sequence for **3**, suggesting that steric, rather than electronic, forces control the isomeric structures of the more highly cyclopentadienyl substituted complexes.

The *g* values and hyperfine parameters derived from EPR spectra of the 49 e^- radicals are consistent with those found by previous workers for isoelectronic clusters. Additional features are found, however, in frozen solutions of the radicals which are interpreted in terms of dimers which are strongly exchange-coupled.

Experimental Section

Chemicals. Standard Schlenck procedures (under N_2) were used in preparations of the organometallic compounds. Solvents were dried and distilled: CH_2Cl_2 and 1,2-$C_2H_4Cl_2$ from CaH_2; THF, diethyl ether, and aliphatic and aromatic hydrocarbons from alkali metals. The preparations of $Cp^*Cp'_2Co_3(\mu_3\text{-CO})(\mu_2\text{-CO})_2$ (**2**) and $Cp^*_2Cp'Co_3(\mu_3\text{-CO})(\mu\text{-CO})_2$ (**3**) followed Cirjack and co-workers.[17] Identifications of **2** and **3** were made by IR, ^1H NMR in $CDCl_3$, and electron-impact mass spectrometry (EIMS). $Cp_2Co_2(\mu\text{-CO})_2$ was prepared by the method of Bergman and co-workers,[18] purified by sublimation, and identified by IR spectroscopy (ν_{CO} = 1782 cm^{-1} in CH_2Cl_2).

The various isomers of $Cp_3Co_3(CO)_3$ (**1**) were prepared by photolysis of $CpCo(CO)_2$, after earlier workers.[10] Because the new isomer **1B** was also isolated from this reaction, the precise preparative conditions are given here. A solution of 1.5 mL of $CpCo(CO)_2$[19] in 85 mL of toluene was irradiated for 96 h under a gentle stream of N_2. Toluene was removed at 320 K, leaving a dark brown residue. Column chromatography on a 30 cm long column of alumina II using 1:1 pentane:CH_2Cl_2 resulted in three fast-moving fractions: unreacted red-brown $CpCo(CO)_2$, green $Cp_2Co_2(\mu\text{-CO})_2$, and brown $Cp_3Co_3(CO)_3$. The last of these [630 mg, 12% based on original amount of $CpCo(CO)_2$] is the mixture **1F**/**1T**, apparently identical to the samples described in earlier reports[9−13] (IR in CH_2Cl_2: ν_{CO} = 1957, 1843, 1801, 1756, 1701 cm^{-1}; ^1H NMR in $CDCl_3$: δ 4.88; EIMS at 40 eV: molecular ion peak at 456 *m*/*z*).

Two additional brown bands were then eluted with pure CH_2Cl_2. The first section of this overlapped pair was collected and yielded 50 mg (1%) of the new isomer $Cp_3Co_3(\mu\text{-CO})_3$ (**1B**) after solvent evaporation. The last band was not characterized.

Complex **1B** was identified by IR spectroscopy in THF (ν_{CO} = 1839, 1784 cm^{-1}), ^1H NMR in $CDCl_3$ (δ = 5.05), EIMS at 40 eV (molecular ion peak at 456 *m*/*z*), elemental analysis [Robertson Laboratories, C: 47.35 (calcd, 47.40), H: 3.08 (calcd, 3.32)], and X-ray crystallography. Crystals suitable for the latter were grown by dissolving **1B** in a small amount of CH_2Cl_2 and allowing the solvent to evaporate slowly at 273 K under N_2. Details of the structure were discussed earlier.[14]

Electrochemistry. The electrochemical procedures are mostly as described earlier.[20] The experimental reference electrode in these studies was a AgCl-coated silver wire, separated from the solution by a fine frit. However, all potentials in this paper are referenced to the ferrocene/ferrocenium couple (Fc). In practice, since the ferrocene oxidation occurred near those of the analytes, cobaltocenium was used as an internal standard, added to the analyte solution as the [PF_6] salt at an appropriate point. Conversion of the experimental potentials to the Fc scale was made by noting that the formal potential of Cp_2Co^+/Cp_2Co in CH_2Cl_2 is −1.33 V vs Fc.[21] Formal potentials are approximated as

(15) If comparing the present paper with the two recent calculational papers of refs 5 and 6, note the following equivalancies in isomer designations (present paper/ref 5/ref 6): **B**/$\mathbf{E}_3$/**A**; **T**/$\mathbf{TE}_2$/**B**; **F**/$\mathbf{FE}_2$/**D**.

(16) Shapley, J. R.; Adair, P. C.; Lawson, R. J. *Inorg. Chem.* **1982**, *21*, 1701.

(17) Cirjack, L. M.; Huang, J.-S.; Zhu, Z.-H; Dahl, L. F. *J. Am. Chem. Soc.* **1980**, *102*, 6626.

(18) ν_{CO} for $Cp_2Co_2(\mu\text{-CO})_2$: 1790 cm^{-1} in THF, 1805 cm^{-1} in petroleum ether, see: Schore, N. E.; Ilenda, C. S.; Bergman, R. G. *J. Am. Chem. Soc.* **1977**, *99*, 1781. The value in petroleum ether was reported as 1798 cm^{-1} in ref 11.

(19) Rausch, M. D.; Genetti, R. A. *J. Org. Chem.* **1970**, *35*, 3888.

(20) Chin, T. T.; Geiger, W. E.; Rheingold, A. L. *J. Am. Chem. Soc.* **1996**, *118*, 5002.

(21) Connelly, N. G.; Geiger, W. E. *Chem. Rev.* **1996**, *96*, 877.

Table 1. Potentials[a] of One-Electron Couples of Tricobalt Cluster Complexes in CH_2Cl_2/0.1 M $[NBu_4][PF_6]$ vs $Cp_2Fe/[Cp_2Fe]^{+}$ [b]

complex	symbol	$E_{1/2}(1+/0)$ (V)	$E_{1/2}(0/1-)$ (V)	$E_{1/2}(1-/2-)$ (V)
$Cp_3Co_3(\mu\text{-}CO)_3$	**1B**[c]	−0.08	−1.34	−2.41
$Cp_3Co_3(\mu_3\text{-}CO)(\mu\text{-}CO)_2/Cp_3Co_3(\mu\text{-}CO)_2(CO)$	**1F**/**1T**[d]	−0.25	−1.54	
$Cp^*Cp'_2Co_3(\mu_3\text{-}CO)\ (\mu\text{-}CO)_2$	**2**[e,f]	−0.43	−1.90	
$Cp^*_2Cp'Co_3(\mu_3\text{-}CO)\ (\mu\text{-}CO)_2$	**3**[e]	−0.59	−2.10	

[a] Cp = cyclopentadienyl, Cp′ = methylcyclopentadienyl, Cp* = pentamethylcyclopentadienyl. [b] $E_{1/2}$ values from CV scans: $E_{1/2} = (E_{pa} + E_{pc})/2$. [c] T = ambient. [d] T = 243 K. [e] T = 253 K. [f] An irreversible oxidation of multielectron height was also observed at $E_{pa} = +0.29$ V ($\nu = 0.2$ V/s).

$E_{1/2}$ [= $(E_{pc} + E_{pa})/2$], where E_{pc} and E_{pa} are the cathodic and anodic peak potentials, respectively, from cyclic voltammograms. Voltammetric diagnostics followed the strategies recently summarized.[22] IR spectroelectrochemistry was carried out with an IRTTLE cell (IRTTLE = IR-transparent thin layer electrode, NaCl windows) using CH_2Cl_2/0.2 M $[NBu_4][PF_6]$ as electrolyte and a gold-minigrid working electrode.[23] Digital simulations of cyclic voltammetry responses were carried out using the explicit finite difference method of Feldberg.[24]

Spectroscopy. NMR spectra were obtained using a 270-MHz Bruker spectrometer. IR spectra were acquired with a Mattson Polaris FTIR spectrometer operating at a resolution of 2 cm^{-1}. Variable-temperature IR spectra of the mixture **1F**/**1T** were recorded on solutions about 2 mM in metal carbonyl complex in an IRTTLE cell with the electrodes disconnected. Temperatures ranging from 299 to 191 K were obtained by varying the rate at which cold nitrogen was blown into the sample chamber and measured by monitoring a thermocouple mounted in the cell body. The cell was allowed to stabilize for 15−30 min before recording spectra at a given temperature (precision: ±1−2°).

EPR spectra were recorded on a modified Varian E-4 spectrometer using DPPH as a *g*-value standard. Most spectra were obtained on frozen (77 K) solutions taken from bulk electrolyses. Sampling of the electrolytic solution was accomplished by transferring it to an EPR tube using a cold syringe, followed by quenching of the tube in liquid nitrogen, all inside a controlled atmosphere box. Chemical reductions of the clusters were accomplished using the strong 1 e^- reducing agent (η^6-C_6Me_6)FeCp[25] ($E_{1/2}$ = ca. −2.3 V vs Fc).[21] Equimolar stoichiometries of a cluster complex and the reducing agent were added to a sample chamber, loaded under N_2, and then evacuated. After collecting solvent in the sample chamber at 77 K under vacuum, the tube was flame-sealed, allowed to thaw and stand for about 3 min at 208 K (dry ice/acetone), then refrozen for analysis at 77 K. EPR spectra were simulated using a modified version of the program described by Taylor and Bray.[26]

Results

We first describe the redox processes of complexes **2** and **3**, which do not appear to isomerize upon oxidation or reduction, before turning to the more complicated reactions of **1**.

Oxidation and Reduction of Complexes 2 and 3. Electrochemistry. Complexes **2** and **3** each display two reversible 1 e^- transfers: one oxidation and one reduction. Studies of **2** were limited to cyclic voltammetry, the $E_{1/2}$ values for the $47e^-/48e^-$ and $48e^-/49e^-$ couples being, respectively, −0.43 and −1.90 V vs Fc (Table 1).

Cyclic voltammetry of **3** at 253 K in CH_2Cl_2 (Figure 1) was consistent with the electron-transfer series of eq 1 ($E_{1/2} = -0.59$ V for $\mathbf{3}^+/\mathbf{3}$ and −2.10 V for $\mathbf{3}/\mathbf{3}^-$, Table 1), in which both redox processes are diffusion-controlled, chemically reversible, and quasi-Nernstian. Concerning the latter, ΔE_p values of 65−70 mV were routinely found for scan rates of ca. 0.2 V/s for these systems, about the same as found for ferrocene under the same conditions. A second anodic wave, irreversible and of multielectron height, representing the oxidation of $\mathbf{3}^+$ at $E_{pa} = +0.29$ V, was not studied further.

$$\mathbf{3}^+ \overset{e^-}{\rightleftharpoons} \mathbf{3} \overset{e^-}{\rightleftharpoons} \mathbf{3}^- \quad (1)$$

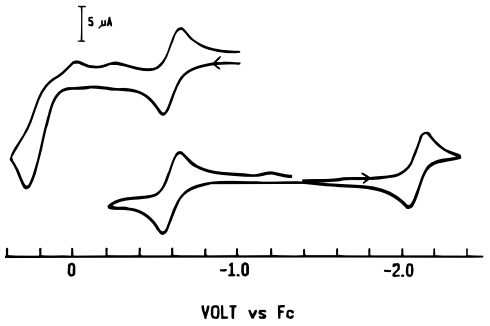

Figure 1. Cyclic voltammograms of 1.0 mM solution of **3** in Ch_2Cl_2/0.1 M $[Bu_4N][PF_6]$ at 253 K, $\nu = 0.2$ V/s. The upper trace shows a scan to more positive potentials.

Bulk electrolyses showed that $\mathbf{3}^-$ and $\mathbf{3}^+$ are stable for at least 1 h in CH_2Cl_2. Exhaustive reduction of **3** at −2.4 V at 223 K produced a brown solution of the anion after passage of 1.0 F/equiv; reoxidation at −1.4 V regenerated the starting material quantitatively except for a small reversible wave at $E_{1/2} = -1.71$ V which may be due to $[Cp^*_2Co_2(\mu\text{-}CO)_2]^{0/-}$.[27a] Solutions of $\mathbf{3}^-$ thus produced in either CH_2Cl_2 or 1:1 CH_2Cl_2:$C_2H_4Cl_2$ were sampled for EPR analysis (vide infra).

Bulk oxidation of **3** ($E_{appl} = -0.3$ V) at 273 K released 1.2 F/equiv and produced voltammetry consistent with quantitative conversion to $\mathbf{3}^+$. Rereduction of $\mathbf{3}^+$ at $E_{appl} = -1.4$ V (0.85 F/equiv) produced about 80% reconversion to **3** with a small side product having $E_{pc} = -1.67$ V, close to the potential expected for a $(C_5R_5)Co(CO)_2$ complex.[27b]

Infrared Spectroscopy of $\mathbf{3}^+$ and $\mathbf{3}^-$. Vibrational spectra of the redox products in the metal−CO region were obtained using an IRTTLE cell arrangement with 1 mM **3** in CH_2Cl_2/0.2 M $[NBu_4][PF_6]$ at ca. 250 K. Conversion of **3** to $\mathbf{3}^-$ produced isosbestic points as the electrolysis proceeded (Figure 2, top), establishing the clean conversion of the neutral complex (ν_{CO} = 1803, 1754, 1655 cm^{-1}) to the corresponding monoanion (ν_{CO} = 1731, 1681, 1600 cm^{-1}). Expressing the frequency shift for the product as $\Delta\nu_{CO}$, the two edge-bridging carbonyl bands move to lower frequencies by $\Delta\nu_{CO} = -72$ and −73 cm^{-1},

(22) Geiger, W. E. In *Laboratory Techniques in Electroanalytical Chemistry*, 2nd ed.; Kissinger, P. T., Heineman, W. R., Eds.; Marcel Dekker: New York, 1996; Chapter 23.

(23) Atwood, C. G.; Geiger, W. E.; Bitterwolf, T. E. *J. Electroanal. Chem.* **1995**, *397*, 279.

(24) Feldberg, S. W. In *Electroanalytical Chemistry*; Bard, A. J., Ed.; Marcel Dekker: New York, 1969; p 199.

(25) (a) Astruc, E. *Acc. Chem. Res.* **1986**, *19*, 377. (b) Astruc, D. *Chem. Rev.* **1988**, *88*, 1189.

(26) (a) Taylor, P. C.; Bray, P. J. *J. Magn. Reson.* **1970**, *2*, 305. (b) Rieger, P. H. *J. Magn. Reson.* **1982**, *50*, 485. (c) DeGray, J. A.; Rieger, P. H. *Bull. Magn. Reson.* **1987**, *8*, 95. (d) DeGray, J. A. Ph.D. Dissertation, Brown University, 1987.

(27) (a) The related system $[Cp_2Co_2(CO)_2]^{0/-}$ has a potential of −1.30 V vs Fc in THF.[8b] The product potential of −1.71 V is roughly consistent with substitution of Cp by Cp* at both metals. (b) Connelly, N. G.; Geiger, W. E.; Lane, G. A.; Raven, S. J.; Rieger, P. H. *J. Am. Chem. Soc.* **1986**, *108*, 6219.

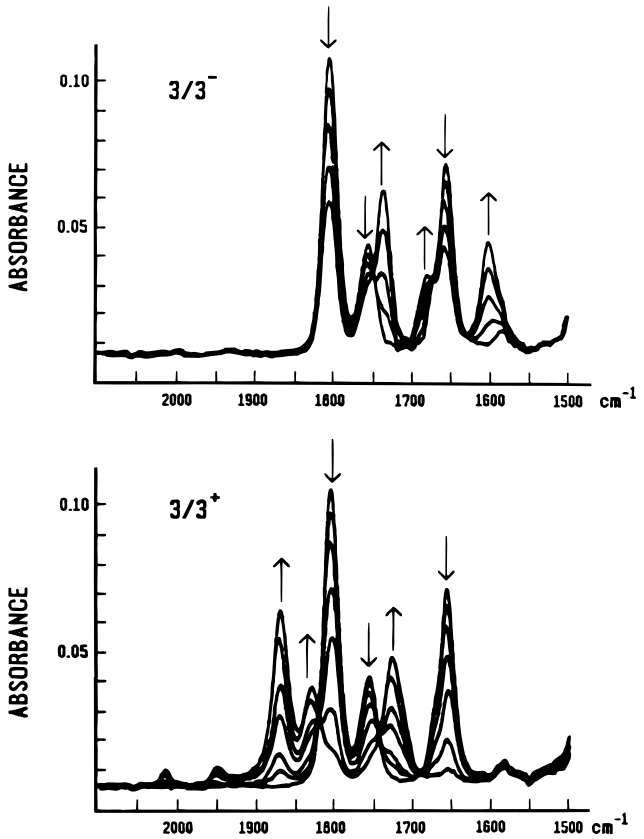

Figure 2. IR spectroelectrochemistry of the reduction (top) and oxidation (bottom) of 1 mM **3** in CH_2Cl_2 at 243 K. Arrows show direction of change upon application of potential, $E_{appl} = -2.4$ V (top), -0.2 V (bottom).

Table 2. Carbonyl Stretching Frequencies for Tricobalt Clusters in CH_2Cl_2

complex	charge on complex	T (K)	absorption bands (cm^{-1})
1B	0	223	1839, 1785
1B	1−	223	1756, 1697
3	1+	243	1870, 1830, 1727
3	0	243	1803, 1754, 1655
3	1−	243	1731, 1681, 1600
1F/1T	0	295	1958, 1845, 1801, 1756, 1700
1F/1T	0	223	1957, 1836, 1794, 1751, 1696
1F	1−	223	1756, 1703, 1611

whereas the face-bridging carbonyl has $\Delta\nu_{CO} = -55$ cm^{-1} (average shift of all three carbonyls: -67 cm^{-1}) (Table 2).

At 243 K, the oxidation of **3** (Figure 2, bottom) gave carbonyl frequencies of $\mathbf{3}^+$ at 1870, 1830, and 1727 cm^{-1}, $\Delta\nu_{CO}$ being +67 and +76 cm^{-1} for the edge-bridging ligands and +72 cm^{-1} for the face-bridging carbonyl (average shift +72 cm^{-1}). At the conclusion of the oxidation two small bands at 2017 and 1951 cm^{-1} signaled the presence of $Cp^*Co(CO)_2$ as a minor decomposition product. Both the cation and anion resulting from, respectively, the oxidation and reduction of **3** have carbonyl frequencies consistent with the presence of two edge-bridging and one face-bridging carbonyl groups in the ions. We conclude, therefore, that **3** (and probably also **2**) retains the same isomeric identity through three cluster oxidation states.

Oxidation and Reduction of 1B. Electrochemistry. The C_{3v} isomer $Cp_3Co_3(\mu\text{-}CO)_3$ (**1B**) has three 1 e^- processes in the potential regime studied: two reversible reductions ($E_{1/2} = -1.34$ and -2.41 V) and one partially chemically reversible oxidation ($E_{1/2} = -0.08$ V, Table 1). Bulk electrolysis at the potential of the first reduction confirmed the 1 e^- nature of the process (measd, 0.9 F/equiv) and produced EPR-active solutions of $\mathbf{1B}^-$ (vide infra).

IR spectra of the 49 e^- monoanion $\mathbf{1B}^-$ were obtained by IRTTLE-cell electrolysis at 223 K with $E_{appl} = -2.0$ V. The higher solution viscosity at this low-temperature slowed the electrolysis, which was stopped after a mixture was achieved of about 70% $\mathbf{1B}^-$ and 30% **1B**. Spectral subtraction of the bands of **1B** (1839 and 1785 cm^{-1} at 223 K) gave a spectrum showing the two CO bands of $\mathbf{1B}^-$ (1756 cm^{-1}, 1697 cm^{-1}; Supporting Information Figure S1). The observation of a pair of carbonyl bands establishes that the anion $\mathbf{1B}^-$ retains approximate C_{3v} symmetry. The value of $\Delta\nu_{CO}$ is -78 cm^{-1} for both bands (Table 2).

The oxidation of **1B** is a 1 e^- process (bulk coulometry: 0.9 F/equiv at $T = 223$ K), but the monocation $\mathbf{1B}^+$ is unstable, undergoing isomerization to $\mathbf{1T}^+$. The onset of chemical reversibility in CV scans of **1B** at ambient temperatures comes at ca. 0.3 V/s. After scanning through the oxidation of **1B**, a (reversible) product wave is seen on the reverse sweep with $E_{1/2} = -0.26$ V, the same potential measured for the oxidation of **1T** (vide infra). Digital simulations (Supporting Information Figure S2) allowed determination of the half-life of $\mathbf{1B}^+$ as 0.5 s at 223 K. We therefore write the redox behavior of the C_{3v} isomer as eq 2:

$$\mathbf{1T}^+ \xleftarrow{1.6\ s^{-1}} \mathbf{1B}^+ \overset{e^-}{\rightleftharpoons} \mathbf{1B} \overset{e^-}{\rightleftharpoons} \mathbf{1B}^- \overset{e^-}{\rightleftharpoons} \mathbf{1B}^{2-} \qquad (2)$$

This scheme is supported by electrolysis experiments in which oxidation of **1B** followed by reduction of the anodic products at $E_{appl} = -0.5$ V gave a solution with voltammetric waves equivalent to those of **1F**/**1T**. The oxidation product of **1B** could not, unfortunately, be identified by IR spectroelectrochemistry since the oxidation product(s) appeared to passivate the gold minigrid working electrode.

The 1F/1T Mixture: Characterization by IR. IR spectroscopy was employed to quantify the amounts of isomers **1T** and **1F** in different solvents. Qualitative measurements were reported in a number of earlier studies,[9−13] but current instrumentation is more suitable for quantitative work. Our results show that both isomers (**1T** and **1F**) are present in solvents both nonpolar (benzene) and moderately polar (CH_2Cl_2 and THF). Variable-temperature measurements were used to estimate the equilibrium constant of eq 3 in CH_2Cl_2 between 299 and 191 K.

$$K_{F/T} = [\mathbf{1F}]/[\mathbf{1T}] \qquad (3)$$

Mixtures of **1T** and **1F** are characterized by five absorptions in the CO region since the two isomers have three bands each (Table 2 and Figure 3) and the bands at ca. 1800 cm^{-1} coincide. The bands at 1840 and 1698 cm^{-1} (assigned to **1F**) increase at lower temperatures compared to those of **1T** at 1958 and 1753 cm^{-1}. The intensity ratio A_{1840}/A_{1753} was used to calculate $K_{F/T}$, assuming $\epsilon_{1840} = \epsilon_{1753}$.[28] The values of $K_{F/T}$ measured on 2 mM solutions from 299 to 191 K are given in Table 3, and the resulting van't Hoff plot (Supporting Information Figure S3) gave $\Delta H° = -4.4$ kJ/mol. At ambient temperatures there is a slight excess of **1T** over **1F**, but this is reversed at temperatures below about 260 K.

The proton NMR spectrum of $CDCl_3$ solutions of **1F**/**1T** consists of a sharp singlet at $\delta = 4.88$ ppm, showing that interconversion of the two isomers is fast on the NMR time scale.

(28) An assumption of this nature is necessary owing to the unavailability of pure solutions of either isomer. We chose the bands at 1840 and 1753 cm^{-1} because they both arise from absorptions of doubly-bridging carbonyls.

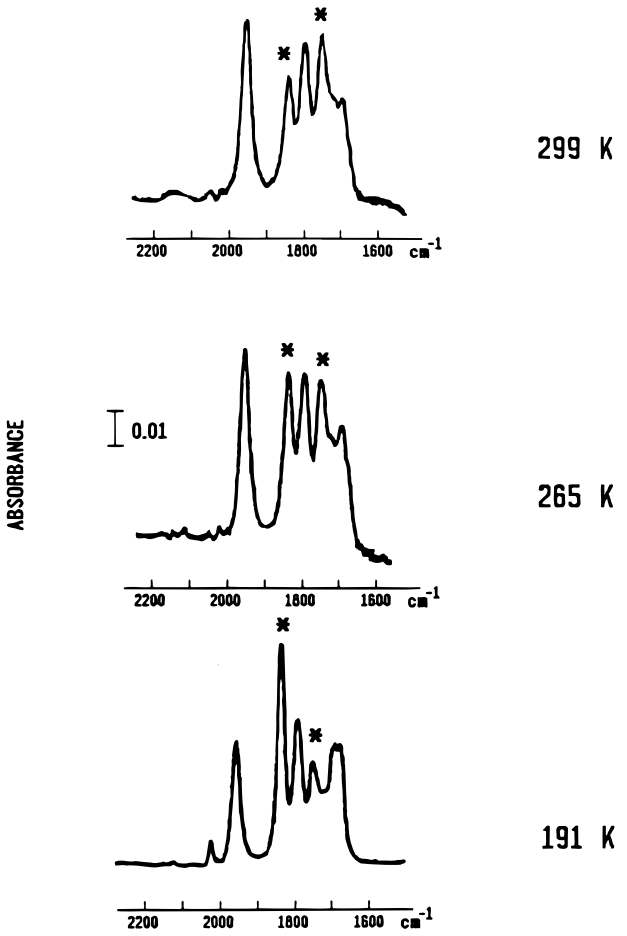

Figure 3. Variable-temperature IR data on a 2.5 mM solution of the mixture **1F**/**1T** in CH_2Cl_2. Asterisks mark the two bands used for the calculation of K_{FT} of Table 3, 1840 cm^{-1} for **1F**, 1753 cm^{-1} for **1T**.

Table 3. Apparent Equilibrium Constants $K_{F/T}$ as a Function of Temperature

T (K)	$K_{F/T}$	T (K)	$K_{F/T}$
299	0.78	216	1.62
290	0.89	201	1.95
262	1.09	192	2.13

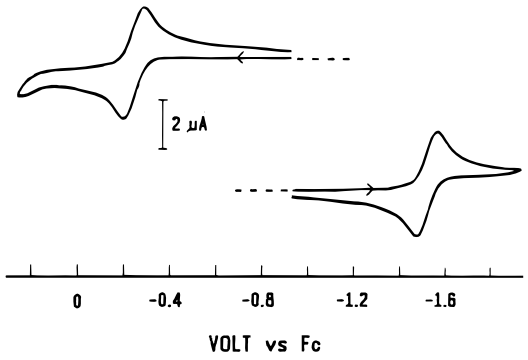

Figure 4. Cyclic voltammograms of 1.0 mM solution of **1F**/**1T** in CH_2Cl_2/0.1 M $[Bu_4N][PF_6]$ at 243 K, $\nu = 0.3$ V/s. The zero current levels for the two scans are shown as dotted lines.

The 1F/1T Mixture: IR Spectroelectrochemistry. Cyclic voltammetry of **1F**/**1T** in CH_2Cl_2 shows a pair of essentially Nernstian 1 e^- waves over a range of temperatures (Figure 4): one reduction ($E_{1/2} = -1.54$ V) and one oxidation ($E_{1/2} = -0.25$ V). The anodic product is stable for only a few seconds at 243 K, CV scan rates above 0.25 V/s being necessary to achieve

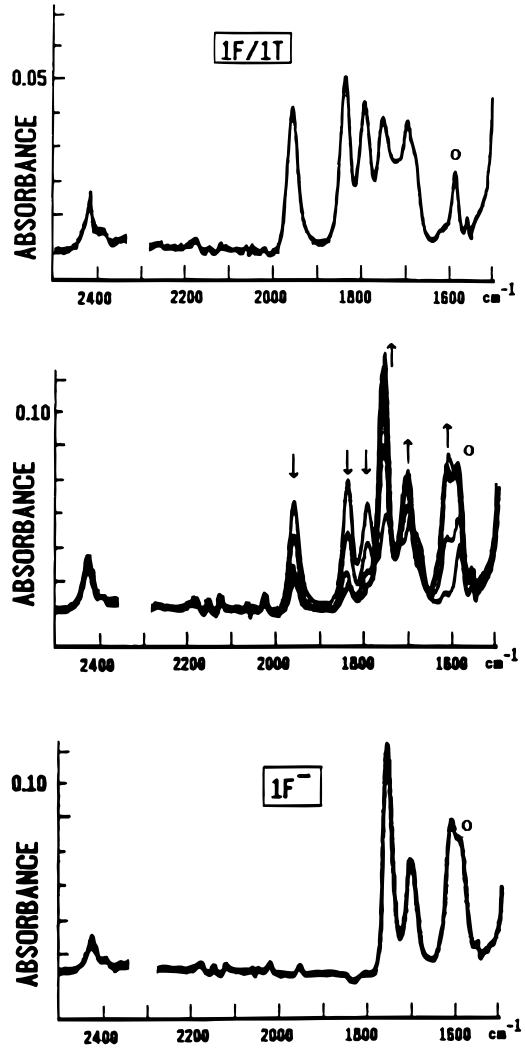

Figure 5. IR spectroelectrochemistry of the reduction of the mixture **1F**/**1T** to produce $\mathbf{1F}^-$. Top: 1 mM solution prior to electrolysis. Middle: spectral changes with the time when $E_{appl} = -1.8$ V. Bottom: after exhaustive reduction. The circle marks a spectral interference that does not arise from either **1F**/**1T** or its electrolysis product(s).

complete chemical reversibility. The 1 e^- reduction product, $[Cp_3Co_3(CO)_3]^-$, was detected by IRTTLE spectroscopy after the mixture of neutral isomers was reduced at 223 K in CH_2Cl_2 at $E_{appl} = -2$ V. As shown in Figure 5, the five bands for **1F**/**1T** decrease as the electrolysis proceeds and three new absorptions appear at 1756, 1703, and 1611 cm^{-1}. The last of these certainly establishes the presence of a face-bridging carbonyl in the monoanion. None of the absorptions is consistent with an anion having a terminal carbonyl, so it is concluded that the mixture of **1F** and **1T** in the 48-electron system converts entirely to $\mathbf{1F}^-$ at the 49-electron stage. No other product bands were apparent, and reoxidation of $\mathbf{1F}^-$ at $E_{appl} = -1$ V regenerated the original spectrum quantitatively. The three bands of $\mathbf{1F}^-$ are shifted an average of -85 cm^{-1} from those of **1F** (Table 4). Regarding the oxidation process, IR spectroelectrochemistry confirmed the CV-based conclusion that the 47 e^- cluster is unstable. Oxidation of **1F**/**1T** at 223 K in CH_2Cl_2 using $E_{appl} = 0$ V gave only peaks due to starting material and apparently neutral decomposition products [those identified were $CpCo(CO)_2$ at 2030 cm^{-1} and 1960 cm^{-1} and $Cp_2Co_2(\mu\text{-}CO)_2$ at 1782 cm^{-1}].

The 1F/1T Mixture: Voltammetry. As stated above, the mixture of neutral isomers has CV characteristics that are not

Table 4. Electron-Transfer Induced Changes in Carbonyl Stretching Frequencies, $\Delta\nu_{CO}$, for Trinuclear Cluster Compounds[a]

edge-bridging CO			
type 1[b]	type 2[c]	face-bridging CO	terminal CO
78 (**1B**/**1B**$^-$)	67 (**3**$^+$/**3**)	72 (**3**$^+$/**3**)	60[d]
83 (**1B**/**1B**$^-$)	76 (**3**$^+$/**3**)	55 (**3**/**3**$^-$)	
85 (**1B**/**1B**$^-$)	72 (**3**/**3**$^-$)	85 (**1F**/**1F**$^-$)	
	80 (**1F**/**1F**$^-$)	55[e]	
	91 (**1F**/**1F**$^-$)		
av (rsd) 82 ± 4	78 ± 8	66 ± 15	60

[a] $\Delta\nu_{CO} = \nu_{CO}$ of higher oxdn state − ν_{CO} of lower oxdn state (in cm^{-1}). [b] One CO ligand on a M−M edge. [c] Two CO ligands on a M−M edge. [d] Neutral complex minus anion for $[Co_3(CO)_9(\mu_3\text{-CR})]^{0/1-}$ (ref 40). [e] Cation minus neutral complex for $[Cp^*_3Co_3(\mu\text{-CO})(\mu_3\text{-NH})]^{1+/0}$ (Bedard, R. L.; Rae, A. D.; Dahl, L. F. *J. Am. Chem. Soc.* **1986**, *108*, 5924).

at all suggestive of the presence of more than one redox component. Except for the unlikely scenario[29] that the $E_{1/2}$ potentials of **1F** and **1T** are virtually identical, the reason for this apparent inconsistency lies in the rapid interconversion of **1F** and **1T** (NMR data, vide ante) during the CV scan. The potential of the 48 e$^-$/49 e$^-$ couple **1F**/**1F**$^-$ can be predicted based on the values measured for **2** and **3**, modified by the substituent effect for substitution of $-CH_3$ by $-H$ in the cyclopentadienyl rings. Using a value of $\Delta E_{1/2} = 0.045$ V per substitution,[30] the predicted $E_{1/2}$ for **1F** is −1.57 V, very close to the experimental value of −1.54 V for the isomeric mixture. We expect the potential of **1T** to be negative of that of **1F** owing to the lower electron-withdrawing power of a terminal CO in the latter complex.[29] The cathodic response at −1.54 V must be rationalized, therefore, by a CE mechanism (eqs 4 and 5)

$$\mathbf{1T} \underset{k_b}{\overset{k_f}{\rightleftharpoons}} \mathbf{1F} \tag{4}$$

$$\mathbf{1F} + e^- \rightleftharpoons \mathbf{1F}^- \tag{5}$$

in which k_f of eq 4 is large. As the more easily reduced isomer (presumably **1F**) is consumed in the reduction, **1T** converts to **1F**, feeding the cathodic process until both isomers are consumed. Importantly, therefore, the conversion of **1T** to **1F**$^-$ (demonstrated by IR spectroelectrochemistry) does not require the intermediacy of **1T**$^-$. Still, it is likely that structure **F** is the thermodynamically favored isomer in the 49 e$^-$ complex. Otherwise, one would have to posit that the isomerization of **1F**$^-$ is much slower than that of **1F**, an unlikely scenario given the known tendency of odd-electron counts to greatly accelerate carbonyl isomerizations.[8]

The anodic process at $E_{1/2} = -0.25$ V must also be considered in terms of the fast interconversion between the two electrochemical reactants **1F** and **1T**. The current functions, $i_p/v^{1/2}$, were equal for this anodic reaction and the previously discussed cathodic one at −1.54 V, showing that the oxidation wave is also of full 1 e$^-$ height. In contrast with the cathodic reaction, however, we get no spectroscopic clues as to the isomeric identity of the oxidation product since the 47 e$^-$ cation decomposes on the spectroelectrochemical time scale (vide ante). Lacking spectroscopic evidence, we turn to consideration of the electrochemical potentials for further analysis of the anodic reaction.

By analogy to complexes **2** and **3**, isomers of the type **F** are assumed to have difference of ca. 1.49 V separating the 47 e$^-$/48 e$^-$ and the 48 e$^-$/49 e$^-$ couples (1.47 V for **2**, 1.51 V for **3** (Table 1)). The $E_{1/2}$ value for **1F**/**1F**$^+$ predicted from this analogy is −0.05 V, about 200 mV positive of the observed value of −0.25 V, leading to the conclusion that the anodic wave arises from the oxidation of **1T** rather than **1F**.[31]

Scheme 1

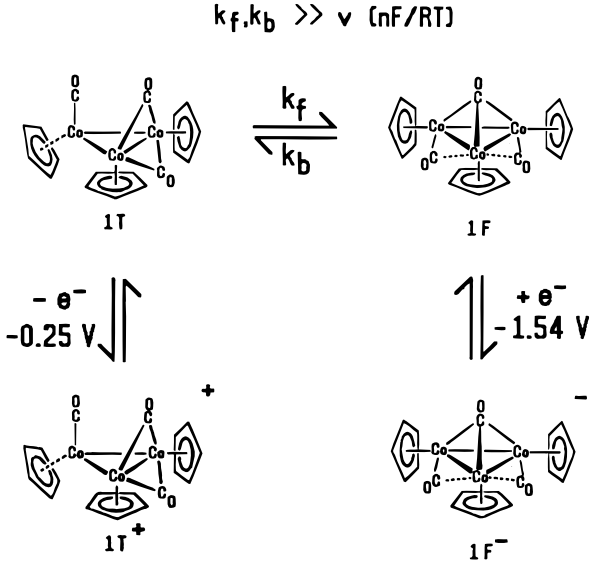

We thus conclude that the reduction and oxidation waves of **1F**/**1T** arise from the redox processes of two different isomers: **1F** for the reduction to the 49 e$^-$ cluster (**1F**$^-$) and **1T** for the oxidation to the 47 e$^-$ cluster (**1T**$^+$), both through CE mechanisms (eqs 4 and 5 for the former, eqs 4 and 6 for the latter) (Scheme 1).

$$\mathbf{1T} \rightleftharpoons \mathbf{1T}^+ + e^- \tag{6}$$

EPR Spectra of 49 e$^-$ Systems 3$^-$, 1B$^-$, and 1F$^-$. The 49 e$^-$ anions of these clusters are EPR-active. Spectra were obtained from samples prepared either by bulk cathodic electrolysis of the 48 e$^-$ precursors in $CH_2Cl_2/C_2H_4Cl_2$ or by their reduction using equimolar $(C_6Me_6)FeCp$ as a reducing agent[21] in THF. The general spectral features are the same for both methods of radical production, but the resolution of fine structure was generally superior for the electrochemically prepared samples, so only those data will be discussed. Fluid solution spectra, when observed, were very broad and did not contribute to our understanding of the frozen-solution spectra which are discussed below. The 47 e$^-$ monocation **3**$^+$ gave a single broad (peak-to-peak ≈ 150 G width) frozen solution resonance at $g = 2.000$.

The EPR spectrum of **1B**$^-$ is shown in Figure 6a. The major parallel features observed in the spectrum are consistent with

(29) The electron-withdrawing power of bridging carbonyls is considerably greater than that of terminal carbonyls, accounting for the demonstrably higher $E°$ potentials in 1 e$^-$ reactions of cluster compounds with bridging CO ligands. See refs 8 and 9 for leading references concerning this point.

(30) This value is obtained by inspection of the potentials of the related clusters **2** and **3**, which differ in the methyl substitution on the Cp rings, but it is also consistent with considerable previous literature. For leading references, see: Merkert, J. W.; Geiger, W. E.; Attwood, M. D.; Grimes, R. N. *Organometallics* **1991**, *10*, 3545.

(31) The apparent $E_{1/2}$ values are affected by the equilibrium between the neutral 48 e$^-$ isomers, but the shifts from the true $E_{1/2}$ values for **1F**/**1F**$^+$ and **1F**/**1F**$^-$ are such that the difference between the two observed waves would increase, not decrease. For example, consider the reduction of **1F** which is in equilibrium with **1T**. In this case, $E_{1/2}(\text{obsd}) = E_{1/2}(\mathbf{1F}/\mathbf{1F}^-) - RT/F \ln(1 + K_{F/T}^{-1})$.[37] At $T = 243$ K, using $K_{F/T} \approx 1.3$ (Table 3), a shift of ≈−40 mV is predicted for $E_{1/2}(\text{obsd}) - E_{1/2}$ (**1F**/**1F**$^-$). The shift in the oxidation process will be ≈+ 40 mV from $E_{1/2}$ (**1F**/**1F**$^+$). We also note that square wave analyses (refs 37 and 38) show that a negative shift of the oxidation wave from $E_{1/2}$ (**1F**/**1F**$^+$) cannot be produced by rapid formation of **1T**$^+$ from the oxidation of **1F** if the $E_{1/2}$ of the **1T**/**1T**$^+$ couple is positive of $E_{1/2}$ (**1F**/**1F**$^+$).

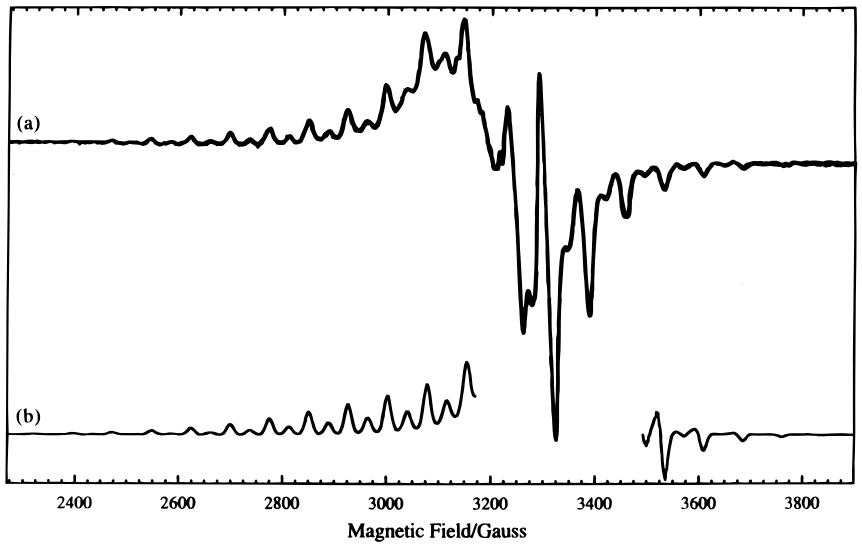

Figure 6. (a) EPR spectrum recorded at 77 K in CH_2Cl_2:$C_2H_4Cl_2$ of solution prepared by cathodic electrolysis of 1 mM **1B**. (b) Simulated spectrum employing the parameters given in Table 5.

hyperfine coupling to three equivalent ^{59}Co nuclei ($I = {}^7/_2$): 22 features with intensity ratios 1:3:6:10:15:21:28:36:42:46:48: 48:46:.... Only 18 features are clearly resolved so that the center is somewhat ambiguous. However, the best fit to the amplitude ratios is obtained with $g_{||} = 2.133 \pm 0.001$, $A_{||} = (75.3 \pm 0.2) \times 10^{-4}$ cm^{-1}. The perpendicular region of the spectrum is poorly resolved with no clearly assignable features. Computer simulations (see below) suggest $g_\perp \approx 2.00$, $A_\perp < 4 \times 10^{-4}$ cm^{-1}. The most striking aspect of the spectrum is the appearance of extra features, located midway between each pair of parallel features. We have considered a variety of hypotheses to explain the extra features: (1) The two sets of features correspond to two isomers or conformers of **1B**$^-$. This would require that the parallel coupling constant in gauss, $A_{||}/g_{||}\mu_B$, be identical for the two structures, with the difference in the centers of the parallel hyperfine patterns, $h\nu/\mu_B(1/g_{||} - 1/g_{||,2})$, equal to exactly half of $A_{||}/g_{||}\mu_B$; such a coincidence is hardly credible. (2) The major and extra parallel features represent two components of the g matrix with identical hyperfine couplings. Not only is it very unlikely that two components of the hyperfine matrix would be precisely the same, but the interior features should have a "divergence shape", which they do not. (3) The extra features are due to ^{13}C coupling. Although the features have approximately the right amplitudes for coupling to 15 equivalent carbons, the required coupling would have to be almost exactly the same as $A_{||}^{Co}$ and thus unbelievably large. (4) The Co nuclei are nonequivalent. The observed intensity ratios cannot be reproduced even approximately by any combination of coupling constants. (5) The extra features are due to noncoincident hyperfine axes. Noncoincidence does indeed result in extra lines, but they are never systematically arranged midway between the main lines; a small portion of the spectrum, but not its whole, can be fitted in this way. Indeed, we can conclude from examination of this hypothesis that the hyperfine parallel axes are coincident with or at most 10−15° away from the g-matrix parallel axis, necessarily the C_3 axis. (6) The extra features correspond to "forbidden" transitions allowed by quadrupole coupling or hyperfine anisotropy. Although these phenomena may indeed allow transitions in which both the electron and nuclear spin flip, resulting in extra lines between the allowed lines, their transition probabilities are proportional to $\sin^2(2\theta)/K$,[4] where θ is the angle between the field and the parallel axis and K is the angle-dependent coupling constant.[32] For large A_z, the transition probability is vanishingly small for orientations close to the parallel axis. Simulations show forbidden lines in the perpendicular region but not in the parallel region. Allowing noncoincident hyperfine axes complicates matters but does not change the qualitative conclusions.

The spectrum has the appearance of the superposition of a "normal" Co_3 spectrum with 22 parallel features and the spectrum of a Co_6 species with 43 parallel features having exactly half the coupling. The latter is precisely what is expected if two Co_3 species were associated, with coincident parallel axes. The "dimer" spectrum therefore arises from exchange between the 49 e$^-$ cluster anion and, most likely, a 48 e$^-$ neutral precursor which is proximate to it.[33] An arrangement such as shown in Figure 8 would account for our observations. This hypothesis is supported by the amplitude ratios observed in the spectra. The amplitudes of the extra features, relative to those of the adjacent normal features, decrease with increasing $|M|$, where $M = m_1 + m_2 + m_3$. This is expected if the normal features are due both to monomer and dimer and the extra features only to the dimer. For three equivalent spin-7/2 nuclei, the degeneracies range from 1 ($M = \pm 21/2$) to 48 ($M = \pm 1/2$), but for six such nuclei, the range is 1 ($M = \pm 21$) to 18 152 ($M = 0$). Thus the dimer contribution to the normal features decreases rapidly with increasing $|M|$, as do the amplitudes of the extra features. The last feature observed with reasonable signal-to-noise corresponds to $M = 17/2$ (6-degenerate) for the Co_3 species or to $M = 17$ (126-degenerate) for the Co_6 species. The feature corresponding to monomer $M = 1/2$ (48 degenerate) or dimer $M = 1$ (17 982-degenerate) in the experimental spectrum has an amplitude 28 times that of the $M = 17/2$ (or 17) feature. Since the approximate expected amplitude ratios from computer simulations[34] are 1:13 for the monomer and 1:113 for the dimer, the observed ratio is consistent with a mixture. The ratios of the amplitudes of five well-resolved extra

(32) Atherton, N. M. *Electron Spin Resonance*; Ellis Harwood: Chichester, U.K., 1973; p 227.

(33) Two 49 e$^-$ clusters may exhibit spectra of the type discussed here if their exchange energy J is much greater than $A_{||}$. For a similar observation involving nitroxide radicals, see: Briere, R.; Dupeyre, R-M.; Lemaire, H.; Morat, C.; Rassat, A.; Rey, P. *Bull. Soc. Chim. Fr.* **1965**, 3290.

(34) The computer simulations account for overlap of spectral features as well as the fact that the absorption for a given M is spread over a range from the position of the parallel feature to the corresponding perpendicular feature so that amplitude ratios are only approximately equal-to-degeneracy ratios.

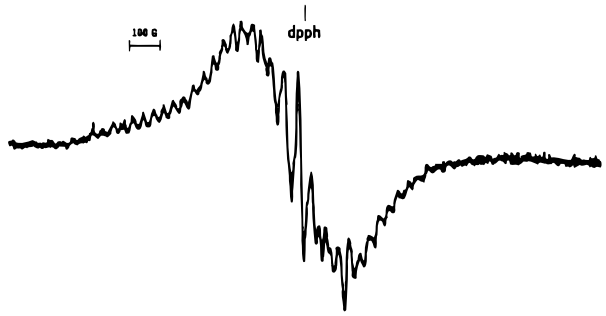

Figure 7. EPR spectrum of $\mathbf{3}^-$, and its apparent dimer produced by cathodic reduction of **3**, in CH_2Cl_2:$C_2H_4Cl_2$ at 77 K.

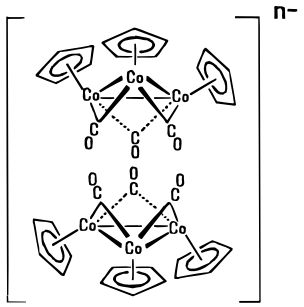

Figure 8. Possible orientation of two clusters in frozen matrix responsible for "dimer" EPR features. *n* may be 1 or 2.

features, due to dimer only, to those of the adjacent major features, due to monomer and dimer, were compared with the corresponding amplitude ratios from computer simulations to estimate the monomer/dimer concentration ratio as 1.6 ± 0.4, i.e., about 40% of $\mathbf{1B}^-$ is present in the frozen solution as a dimer. Adding simulations of the monomer and dimer spectra with this ratio gives the simulation shown in Figure 6b, which gives a good account of the parallel features of the experimental spectrum.[35] Spectra having similar extra features, albeit with lower intensities, have been previously published without comment as to their origin.[36]

A dimer structure such as that shown in Figure 8 is consistent with the EPR data.

Similar spectra are observed for $\mathbf{3}^-$, an anion shown by IR and electrochemistry to be stable as a type-**F** isomer. In this case, however, the amount of the dimer must be larger, leading to normal and extra features that are almost equal in intensity (Figure 7), $A_{||} = 70 \times 10^{-4}$ cm^{-1}.

Comparable results were found yet again for frozen solutions of the other **F**-type anion studied, $\mathbf{1F}^-$. The spectra were of poorer quality because of lower S/N values (Supporting Information Figure S4), but they allow a similar interpretation with $A_{||} = 63 \times 10^{-4}$ cm^{-1}. Table 5 summarizes the quantifiable ESR data.

The cobalt hyperfine splittings are consistent with those reported by others for 49 e$^-$ trinuclear systems of related structure.[39−43] For example, $A_{||}$(Co) values of 66−76 G have been reported for the isoelectronic systems $(\mu_3\text{-S})Co_3(CO)_9$,[39] $[(\mu_3\text{-S})FeCo_2(CO)_9]^-$,[40] and $[(\mu_3\text{-CPh})Co_3(CO)_9]^-$.[40] The related doubly capped system $[(\mu_3\text{-CPh})_2Co_3Cp_3]^-$ has $A_{||} = 83$ G.[41] Detailed treatments[39−41] of these 49 e$^-$ systems show that the extra electron is housed in an orbital of trimetallic character consisting primarily of cobalt $3d_{xy}$ (in-plane) contributions. The same type of orbital seems likely therefore to be the SOMO of each of the three 49 e$^-$ Co_3 radicals investigated in the present study. Since this orbital is antibonding with respect to the metals, it is likely that the Co−Co distances in the 49 e$^-$ clusters are somewhat longer than those in their 48 e$^-$ counterparts.[44]

Table 5. Low-Field Co Hyperfine Splitting and Other EPR Parameters of 49 e$^-$ Radicals in This Study[a]

radical	$A_{||}$(Co) ($\times 10^4$ cm^{-1})	other values
$\mathbf{1B}^-$ [b]	75.3 ($g_{||} = 2.133$)	$g_\perp = 2.02$ $A_\perp < 4 \times 10^{-4}$ cm^{-1}
$(\mathbf{1B}^-)_2$[b]	37.7 ($g_{||} = 2.133$)	$g_\perp = 2.02$ $A_\perp < 4 \times 10^{-4}$ cm^{-1}
$\mathbf{1F}^-$	70 ($g_{||} \approx 2.1$)	
$\mathbf{3}^-$	63 ($g_{||} \approx 2.1$)	

[a] Spectra Recorded at 77 K in 1:1 CH_2Cl_2:$C_2H_4Cl_2$. [b] Simulation parameters for Figure 6b.

Discussion

Identification of Isomers by Voltammetry. The discovery[14] of a third isomer (**1B**) of $Cp_3Co_3(CO)_3$ and the present work quantifying the equilibria between **1F** and **1T** appear to settle the remaining questions of isomer identification which have existed since the first report of this cluster over three decades ago.[9] CV experiments allow the differentiation of isomer **1B** from both **1F** and **1T** because only the latter interconvert on the voltammetric time scale. The voltammetry associated with the mixture **1F**/**1T** illustrates the fact that there may be important chemical transformations concomitant with a "completely reversible" CV wave, as long as those transformations are fast and reversible on the time scale of the voltammetry.[45] In the context of the **1F**/**1T** system and the observation that the Cp resonances of the two isomers are averaged in ^{1}H NMR spectra, CV scan rates of $>10^5$ V/s would likely be necessary to see individual voltammetric peaks for the two isomers. We did not attempt such experiments owing to the unsuitability of THF for ultrahigh scan rates.[46]

We can compare the present results with those obtained by Dessy and co-workers[47] for the reduction of $Cp_3Co_3(CO)_3$ in dimethoxyethane. They reported a partially reversible 1 e$^-$ process yielding an EPR-active sample with ">18 hyperfine lines". Given that their sample was reported to have two closely spaced cathodic waves, it may have contained isomer **1B** as well as the **1F**/**1T** mixture.[48] We previously reported[14] that the anion $[Cp_3Co_3(CO)_3]^-$ fragments in DMF at room temperature to give, exclusively, the dinuclear complex $[Cp_2Co_2(\mu\text{-CO})_2]^-$.

(35) Because of the enormous number of nuclear spin states (262 144) computer simulations treated the hyperfine term of the spin Hamiltonian to first-order only. Since $A_\perp$ is small, the second-order terms are negligible for the parallel features but often are larger than first-order terms for the perpendicular features. Accordingly, we made no attempt to fit the perpendicular region of the spectrum and suppressed this region in the simulation shown in Figure 6b.

(36) Chin, T. T.; Sharp, L. I.; Geiger, W. E.; Rieger, P. H. *Organometallics* **1995**, *14*, 1322, Figure 3a.

(37) Laviron, E. *J. Electroanal. Chem.* **1985**, *186*, 1.

(38) Evans, D. H.; O'Connell, K. M. In *Electroanalytical Chemistry*; Bard, A. J., Ed.; Marcel Dekker: New York, 1986; Vol. 14, p 113 ff.

(39) Strouse, C. E.; Dahl, L. F. *Discuss. Faraday Soc.* **1969**, *47*, 93.

(40) Peake, B. M.; Rieger, P. H.; Robinson, B. H.; Simpson, J. *Inorg. Chem.* **1981**, *20*, 2540.

(41) Beurich, H.; Madach, T.; Richter, F.; Vahrenkamp, H. *Angew. Chem., Int. Ed. Engl.* **1979**, *18*, 690.

(42) Peake, B. M.; Robinson, B. H.; Simpson, J.; Watson, D. J. *Inorg. Chem.* **1977**, *16*, 405.

(43) Enoki, S.; Kawamura, T.; Yonezawa, T. *Inorg. Chem.* **1983**, *22*, 3821.

(44) For leading references see Byers, L. R.; Uchtman, V. A.; Dahl, L. F. *J. Am. Chem. Soc.* **1981**, *103*, 1942.

(45) Geiger, W. E. In *Progress in Inorganic Chemistry*; Lippard, S. J., Ed.; John Wiley and Sons: New York, 1985; Vol. 33, pp 275−283.

(46) Wipf, D. O.; Wightman, R. M. *Anal. Chem.* **1990**, *62*, 98.

(47) Dessy, R. E.; King, R. B.; Waldrop, M. *J. Am. Chem. Soc.* **1966**, *88*, 5112.

Table 6. Long-Lived Isomers of $Cp_3M_3(CO)_3$[a]

cluster electron count	isomer **B**	isomer **F**	isomer **T**
47 e$^-$	**$IrCo_2^+$**	Co_3*$^+$	
	Rh_3^+		**Co_3^+**
48 e$^-$	Co_3	Co_3	Co_3
	Rh_3	Co_3*	Rh_3
	$IrCo_2$	Rh_3*	$IrCo_2$
49 e$^-$	Co_3^-	Co_3*$^-$	
	Rh_3^-	Co_3^-	
	$IrCo_2^-$		

[a] Excluded is the all-terminal CO isomer found in $Cp_3Ir_3(CO)_3$ (see ref 16). Legend: Co_3 = **1**; Co_3* = **3**; Rh_3 = $Cp_3Rh_3(CO)_3$ (ref 8b); $IrCo_2$ = $Cp^*IrCp_2Co_2(CO)_3$ (ref 8c); Rh_3* = $Cp^*_3Rh_3(\mu_3\text{-CO})(\mu\text{-CO})_2$ (ref 51); charge on cluster denoted by superscript.

Changes of CO Frequencies with Cluster Electron Count. Carbonyl stretching frequencies are about 100 cm^{-1} lower in mononuclear complexes for every electron added to the complex.[49] The amount of this shift, $\Delta\nu_{CO}$, appears to be somewhat lower in metal cluster complexes. In the present study $\Delta\nu_{CO}$ varies from a low of 55 cm^{-1} to a high of 90 cm^{-1} for 1 e$^-$ changes; these values are collected in Table 4 along with literature reports for other clusters. Although the average spectral shift for edge-bridging carbonyls is larger than that reported for face-bridging CO ligands, the number of reports is so small that the difference is on the edge of statistical relevance and more values need to be collected before one could make this general conclusion. In the broader sense, it appears that 60−80 cm^{-1} shifts per electron may be expected in the redox reactions of metal−carbonyl clusters.

Electronic Structures of the 49 e$^-$ Anions. The EPR parameters, especially the Co hyperfine splittings, are consistent for the 49 e$^-$ anions listed in Table 4 and those of other 49 e$^-$ trinuclear species differing in the identity of metal, face-bridging ligand, and overall charge (vide ante).[37−41] We conclude that the description of the LUMO of the 48 e$^-$ clusters as being a trimetallic antibonding orbital in the plane of the metal triangle[50] is quite general.

Overview of Favored Isomers for 47 e$^-$ to 49 e$^-$ Trinuclear Clusters. The isomers seen for the trinuclear series $[Cp_3M_3(CO)_3]^m$ (m = 1+, 0, 1−) are organized in Table 6 by electron count and isomer type. Included are the long-lived isomers of $Cp_3Co_3(CO)_3$ (**1**, this work), $Cp^*_2Cp'Co_3(CO)_3$ (**3**, this work), $Cp_3Rh_3(CO)_3$,[8b] and $Cp^*IrCp_2Co(CO)_3$.[8c] The designation "long-lived" refers to isomers which have been detected by either spectroscopy or slow sweep CV (e.g., we do not list [**1B**]$^+$ which has a half-life of ≈0.5 s). An isomer clearly established as thermodynamically favored is listed in boldface.

The all-bridging CO arrangement (isomer **B**) is found for each electron count and with all three metals (Co, Rh, Ir). A structure of this type has been seen to isomerize in only one case, the presently reported 47 e$^-$ cation **1B**$^+$ (to **1T**$^+$). This is consistent with the calculations of ref 6 which concluded that the isomerization barrier is high between isomer **B** and the others owing to the energy required to move a CO ligand to an opposite side of the M_3 triangle. The face-bridging CO ligand of isomer **F** has been observed in clusters of the heavier metals only in the sterically-encumbered $Cp^*_3Rh_3(\mu_3\text{-CO})(\mu\text{-CO})_2$.[51] It is, however, common among the tricobalt clusters. The terminal-CO-containing isomer **T** has been detected spectroscopically only in 48 e$^-$ clusters (as thermodynamically unstable species) and when generated electrochemically as **1T**$^+$ fragments within minutes.

The marked stability of isomer **F** in the electron-transfer sequence **3**$^+$/**3**/**3**$^-$ stands out in these studies. It is expected that the smaller tricobalt cluster would enhance steric effects, so we hypothesize that the origin of the preference for the face-bridging isomer in Co_3 clusters is steric rather than electronic in origin. This conclusion is in concert with the calculations of Mercandelli and Sironi.[6] Still, the degree of kinetic stabilization is remarkable, considering that electron-transfer processes enhance isomerization rates of analogous $IrCo_2$ and Rh_3 complexes by 10^4−10^8.[8]

Finally, the triiridium complexes $Cp_3Ir_3(CO)_3$[52] and (η^5-indenyl)$_3Ir_3(CO)_3$[53] have been isolated by Shapley and coworkers as the all-terminal CO isomer and as isomer **B**, respectively. Calculations suggest that the isomerization barriers for these isomers are quite high, at least for 48 e$^-$ species.[6] Whether their odd-electron forms interconvert may be worthwhile to investigate.

Acknowledgment. This work was supported by the National Science Foundation (CHE91-16332 and CHE94-16611) and by the donors of the Petroleum Research Fund (PRF-28321-AC3).

Supporting Information Available: Four figures showing IR spectra of **1B**$^-$, digitally-simulated CV scans of the oxidation of **1B**, a van't Hoff plot of the equilibration of **1F** and **1T**, and an EPR spectrum of **1F**$^-$ (4 pages, print/PDF). See any current masthead page for ordering information and Web access instructions.

JA983341+

(48) In ref 47, the table of observed potentials lists for $Cp_3Co_3(CO)_3$ the values of two cathodic features, E_{pc} = −1.8 and −1.6 V vs Ag/Ag$^+$-(dimethoxyethane), of "complex" relation. When converted to the Fc scale by addition of 0.2 V, the potentials are very close to those presently reported in THF, namely $E_{1/2}$ = −1.54 V for **1F**/**1T** and −1.34 V for **1B**. Another possibility for the more positive potential is $Cp_2Co_2(\mu\text{-CO})_2$, a common impurity in the preparation of $Cp_3Co_3(CO)_3$.

(49) Nakamoto, K. *Infrared and Raman Spectra of Inorganic and Coordination Compounds*, 4th ed.; John Wiley: New York, 1986; pp 291−295.

(50) (a) Lauher, J. W. *J. Am. Chem. Soc.* **1978**, *100*, 5305. (b) Schilling, B. E. R.; Hoffman, R. *J. Am. Chem. Soc.* **1979**, *101*, 3456. (c) Mingos, D. M. P., Wales, D. J., Eds. *Introduction to Cluster Chemistry*; Prentice Hall: Englewood Cliffs, NJ, 1990; p 82 and references therein.

(51) Brunner, H.; Janietz, N.; Wachter, J.; Neumann, H.-P.; Nuber, B.; Ziegler, M. L. *J. Organometal. Chem.* **1990**, *388*, 203.

(52) Shapley, J. R.; Adair, P. C.; Lawson, R. J.; Pierpont, C. G. *Inorg. Chem.* **1982**, *21*, 1701.

(53) Comstock, M. C.; Wilson, S. R.; Shapley, J. R. *Organometallics* **1994**, *13*, 3805.